Diagnostics of underwater electrical wire explosion through a time- and space-resolved hard x-ray source

D. Sheftman, D. Shafer, S. Efimov, K. Gruzinsky, S. Gleizer, and Ya. E. Krasik
Physics Department, Technion, Haifa 32000, Israel

(Received 16 July 2012; accepted 3 October 2012; published online 23 October 2012)

A time- and space-resolved hard x-ray source was developed as a diagnostic tool for imaging underwater exploding wires. A ~4 ns width pulse of hard x-rays with energies of up to 100 keV was obtained from the discharge in a vacuum diode consisting of point-shaped tungsten electrodes. To improve contrast and image quality, an external pulsed magnetic field produced by Helmholtz coils was used. High resolution x-ray images of an underwater exploding wire were obtained using a sensitive x-ray CCD detector, and were compared to optical fast framing images. Future developments and application of this diagnostic technique are discussed. © *2012 American Institute of Physics*. [http://dx.doi.org/10.1063/1.4759492]

I. INTRODUCTION

Fast electrical wire explosions in different media (vacuum, gas, water) have been studied extensively for several decades due to the interesting and important physical phenomena (extreme state of matter, various plasma instabilities, etc.) that accompany these wire explosions, and their important applications (bright source of radiation, fast opening switches, etc.).[1–5] Different electrical, optical, spectroscopic, and x-ray diagnostic methods have been developed and used to study and characterize the time-dependent evolution of the exploding matter. Optical diagnostics are effective to measure the radius of the boundary of the exploding wire.[5] However, in the case of underwater electrical wire explosion, there is some uncertainty concerning the accuracy obtained using these techniques because of the optical distortion caused by the shock wave (SW) generated in the water and the compressed water behind it, which is characterized by a varying index of refraction. Shadow and Schlieren techniques have been used to characterize the expanding SW and the density profile of the water in underwater electrical explosions of wires.[6] In addition, Schlieren photography was used to investigate the density profile of exploding wires in vacuum.[7] However, the dense, non-ideal plasma formed in underwater explosions cannot be probed using laser or spectroscopic techniques because of the opacity of a thin plasma layer that forms in the vicinity of the exploding wire, and the large ($>10^{20}$ cm^{-3}) plasma density of the discharge channel.

Numerous studies in the last decade were dedicated to the development of x-pinch x-ray sources.[4] X-pinch is a novel technique used to produce space- and time-resolved, typically soft, x-rays with remarkable quality and resolution. In order to obtain an efficient hot plasma spot in the process of plasma pinching, extremely large currents ($>10^5$ A) are used. Such a process requires large and expensive facilities and long preparation times. In addition, the x-pinch radiation is characterized by relatively soft continuum x-rays (<20 keV). However, in the case of underwater wire explosions, because of the high level of absorption of soft x-rays by water, hard x-rays (>20 keV) are required for the imaging of exploding wires in water. Powerful hard-x-ray sources, which have been developed based on rod-pinch electron beam diodes,[8] have a typical spot of size <1 mm and time duration of several ns. These sources also require very powerful and expensive pulsed generators with output currents of several tens of kA and voltages of several hundreds of kV. Relatively compact pulsed hard x-ray sources, based on x-ray vacuum diodes, were developed in order to produce time- and space-resolved x-ray images.[9] However, these sources are characterized by a spot size of the order of ~1 mm, larger than that required for the investigation of μm scale variations in underwater exploding wires and for accurately determining the size of the wires.

In this paper, we describe an x-ray source that is used to generate an x-ray flux in a high-current vacuum diode based on cone-shaped Tungsten electrodes. The main requirement of this source is the ability to generate x-rays with energy of >20 keV and μm-scale space resolution. In order to achieve such a resolution, the spot size on the anode affected by the electron impact must be significantly less than 1 mm. In addition, the duration of the electron beam should be in the nanosecond timescale. The latter requirement relate to the source of electron emission. In the case of a high-voltage diode, one can expect to obtain the formation of explosive emission plasma which becomes an electron source. This plasma acquires the cathode potential and expands with typical plasma ion sound velocity of 2×10^6 cm/s.[10] Thus, despite the μm-scale initial cathode emission area, within a few nanoseconds the size of the electron source already increases up to tens of μm. The latter would result in an increase in the size of the anode spot where the interaction of electrons with the anode occurs and, consequently, the spatial resolution would be degraded. Finally, rough estimates, accounting the quantum efficiency of the x-ray camera, <1% conversion efficiency of the electron beam energy into x-ray flux and the finite distance between the x-ray source and the exploding wire, showed that the amplitude of the electron beam should be ≥1 kA in order to achieve sufficient contrast of the x-ray image within several tens of microns. In order to obtain

such large amplitude of the electron beam current, the anode-cathode distance should be $\leq$0.7 mm.

In the present experiments, the obtained images of a 0.6 mm diameter Cu wire exploding in water correspond to a space resolution of 0.1 mm and time resolution of 4 ns. The boundary of the exploding wire measured at different instants of the wire explosion by x-ray imaging was compared to the boundary measured from the optical self-light emission of the exploding wire through fast-frame imaging. Results of this comparison show that the boundaries measured using these methods are nearly identical, hence confirming the results presented in Refs. 5 and 11. In addition, an external magnetic field generated by Helmholtz coils was applied in order to decrease the focal spot size of the electron beam on the anode and, respectively, to enhance the image contrast resolution. It is shown that the magnetic field generated by the coils significantly improves the contrast of the images. In addition, the results of numerical simulations show that through the proper choice of experimental parameters it is possible to achieve an x-ray spot size of a few tens of μm at the anode.

II. EXPERIMENTAL SETUP

The x-ray source is based on a compact spiral generator (SG), consisting of 22 turns of strip-line, which is made of a 190 μm-thick and 200 mm-wide Mylar film glued to a 100 mm wide Cu foil, the edges of which are covered by anticorrosion lacque.[12,13] In the experiments, the SG was charged to 11.5 kV and discharged using a low-inductance trigatron-type gaseous switch, generating an output pulse having a $\sim$1 ns rise time and 120 kV voltage amplitude applied to the load. To achieve such a fast rise-time of the output voltage, an additional spark gaseous switch was used at the SG output. The load consisted of a vacuum diode gap of $\sim$1 mm between two point-shaped Tungsten electrodes. The tip of each electrode was $<$3 μm, which allowed electric field enhancement and significant electron emission from the cathode tip. Bremsstrahlung x-ray radiation was produced from the electron impact on the anode. The cathode was placed in a metal holder connected to the high voltage (HV) output of the generator and the anode was placed in a similar holder connected to a calibrated current viewing resistor (CVR). The electrode holders were screwed onto a dielectric cylindrical chamber. This chamber had 4 windows placed with azimuthal symmetry around the diode in order to enable the x-ray flux to exit and for optical observation (see Fig. 1). Two Helmholtz coils were made of dielectric coated Cu wires, which were wrapped around the plastic chamber, symmetrically with respect to the diode gap center. The distance between the coils was $\sim$15 mm, approximately the radius of the coils. Thus, the coils generated a nearly uniform axial magnetic field at the inter-electrode gap. A 0.9 μF capacitor bank charged to 20–30 kV provided a current pulse with a $\sim$2 μs quarter period to the coils. The resulting peak current in each of the coils reached 7–10 kA, corresponding to a 2–3.5 T magnetic field at the center of the diode. The current through the Helmholtz coils was applied for several shots in order to investigate the enhancement of image contrast due to the focusing magnetic field. However, the large pulsed magnetic pressure between Helmholtz coils resulted in damage to the insulating chamber, and thus future additional engineering design is required to avoid this damage. Consequently, most of the shots recorded were performed without the external magnetic field. The plastic chamber was surrounded by a larger grounded metal chamber, which was pumped to a pressure of approximately 0.025 Pa. Plastic windows were placed in the outer chamber wall for optical calibration. The x-ray generator chamber is illustrated in Fig. 1. Using the sealing o-rings of the dielectric chamber for alignment and a specially designed optical imaging system connected to the x-ray generator chamber, the x-ray generator electrodes were adjusted and axially aligned within a $\sim$5 μm deviation. The cathode and anode could be used for several shots; however, during each shot the tips of the electrodes were degraded, resulting in lower quality images during the following shot.

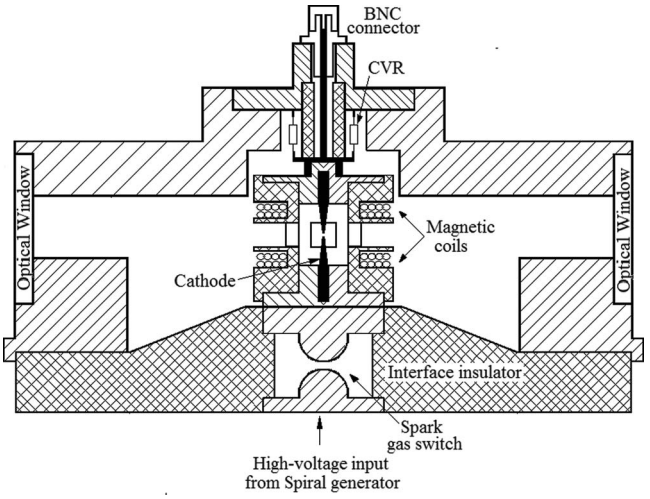

FIG. 1. X-ray generator chamber.

Underwater electrical explosions of Cu wires, 70 mm in length and 0.6 mm in diameter, were carried out inside a water-filled 8 mm-diameter transparent plastic capillary, using the μs-timescale generator described in Ref. 11 (stored

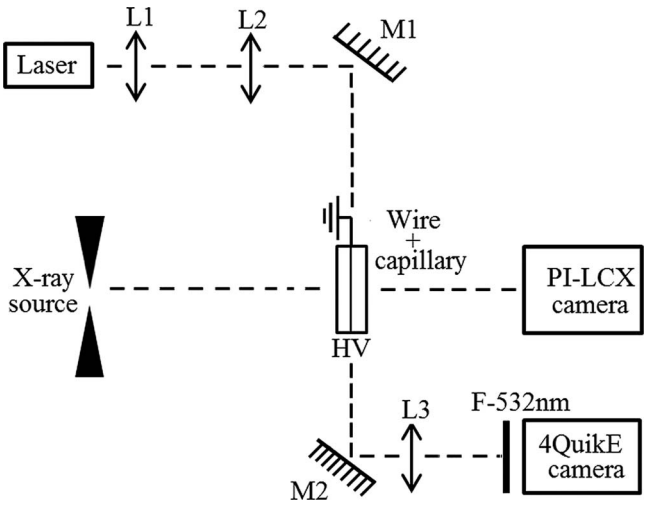

FIG. 2. Experimental setup.

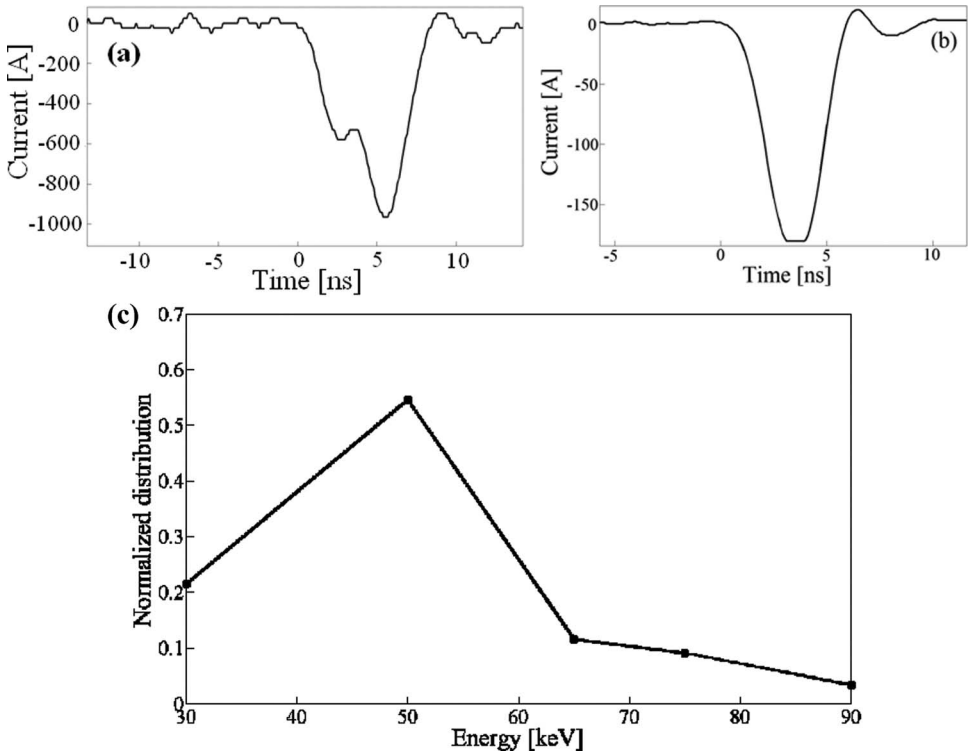

FIG. 3. Electron beam current with Al foil placed in front of the CVR: (a) 10 μm thick and (b) 50 μm thick foil; (c) resulting calculated electron energy distribution.

energy of 4.23 kJ, discharge current during the short-circuit generator shot was ~1.4 μs quarter period with a current amplitude of ~300 kA). The current waveform was measured using a self-integrating Rogowski coil placed around the HV electrode. A schematic presentation of the experimental setup is shown in Fig. 2. The capillary was placed in a stainless steel chamber. The chamber was filled with air at a pressure of 20 psi in order to prevent electrical breakdown between the HV electrode and the chamber walls. Four plastic windows at the outer wall of the chamber were used to enable optical observation and x-ray backlighting of the exploding wire. A 532 nm solid state laser was used for optical calibration of the wire, and a 4 Quik E camera was used to capture the self-light emission of the wire for radius measurement. A PI-LCX x-ray camera, with an x-ray sensitivity range of 0.7–25 keV, was used to capture x-ray images of the exploding wire.

III. RESULTS

A. Diode characteristics

The energy of the electron beam generated in the diode was characterized using 5 different Al foil filters, 10–100 μm-thick. For the purpose of these measurements, the Tungsten rod and anode holder were removed and instead the foils were placed at the entrance to the CVR perpendicular to the electron beam direction, and connected to the ground. In this case, the cathode was placed approximately 2 mm from the foils and the current of the electron beam passing through the foil and entering the CVR was measured. Each foil corresponds to a minimal energy of electrons capable of passing the foil. Thus, an energy distribution measurement point [see Fig. 3(c)] was derived by subtracting the measured time integrated current, corresponding to the foil of a given energy, from the time integrated current measured using the foil of a

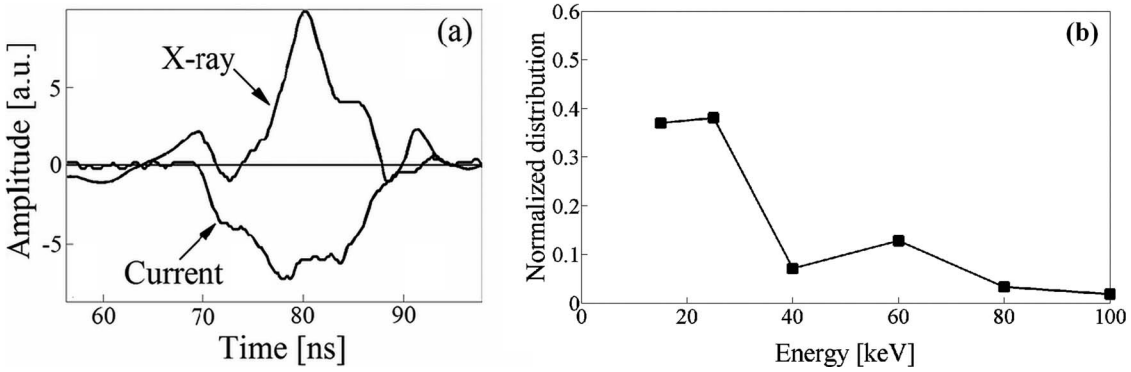

FIG. 4. (a) Waveform of the diode current and x-ray intensity with a 1-cm-thick Al filter placed in front of the PMT; (b) x-ray energy spectrum.

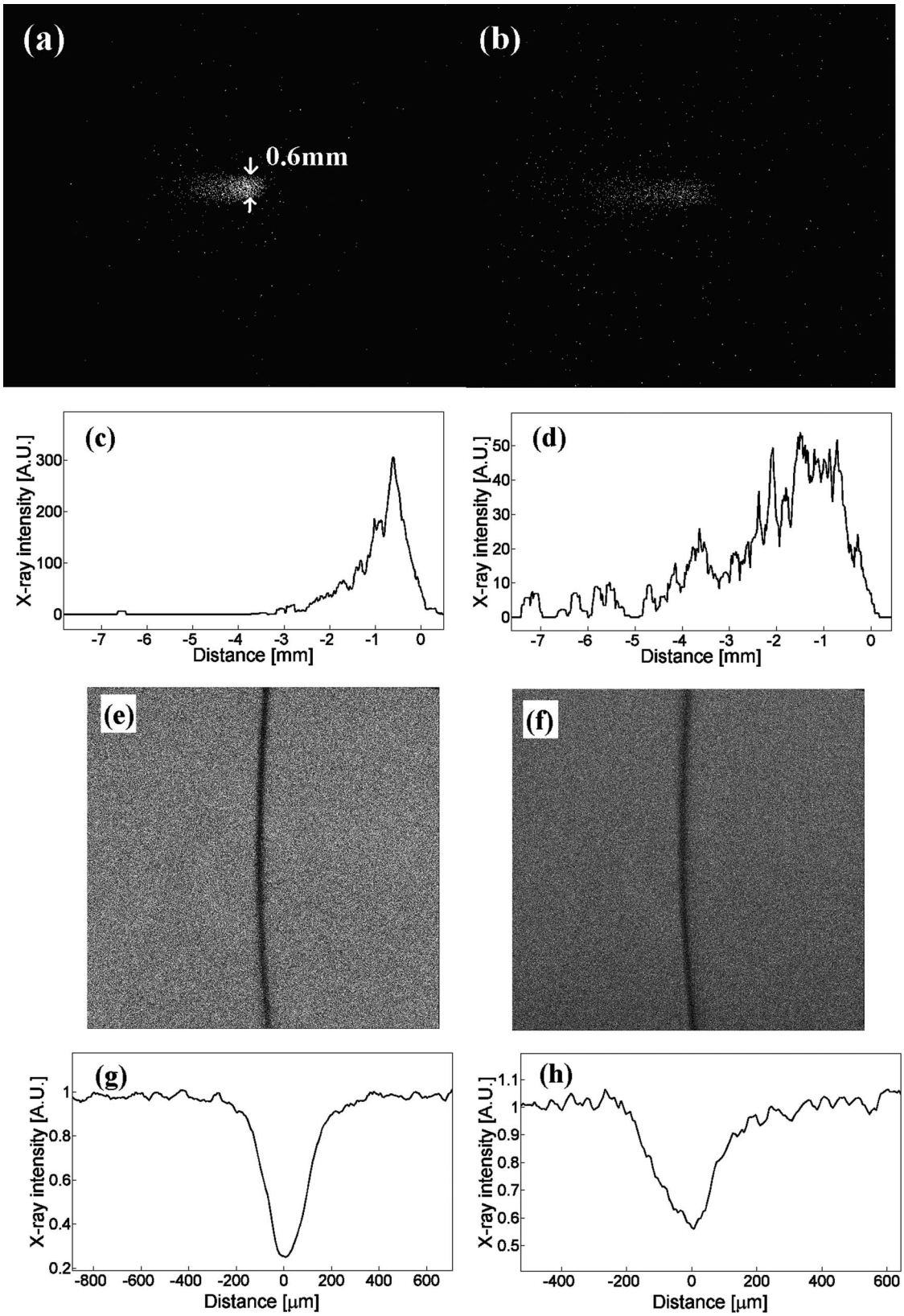

FIG. 5. (a)-(d): Pinhole x-ray image of anode and resulting longitudinal distribution of x-ray intensity with ((a) and (c)) and without ((b) and (d)) application of magnetic field. (e)-(h): Backlighting x-ray image of 0.2 mm W wire and resulting horizontal distribution of x-ray intensity with ((e) and (g)) and without ((f) and (h)) application of magnetic field.

lower energy, and dividing by the energy range between two measurements with subsequent foil thicknesses. The energy corresponding to this calculation is defined as the average between the minimal energies, corresponding to the latter pair of foils. The resulting current waveforms of the electron beam are shown in Fig. 3. For the case of a 10 μm-thick Al foil [see Fig. 3(a)], a ~1 kA current was obtained. Fig. 3(b) shows the electron beam current corresponding to a 50 μm-thick Al foil. It can be seen that the duration of electrons, producing the hard x-ray pulse [Fig. 3(b)], is smaller than the duration of the total electron beam pulse (Fig. 3(a)) which includes "soft" electrons with energies of <30 keV. Indeed, this peak (see Fig. 3(b)) has a time duration of ~4 ns, properly fitting the duration of the x-ray peak shown in Fig. 4(a). The electron energy spectrum presented in Fig. 3(c) shows that the maximum spectrum is obtained for electrons with energy in the range of 45–55 keV.

The energy spectrum of the x-ray photons was measured using a photo-multiplying tube (PMT). For each shot, different Al and Fe filters were placed in front of the PMT in order to measure different energy ranges of the photons. The spectrum was calculated by subtracting subsequent time integrated PMT's voltage waveforms measured using different foils, in a method identical to the one above describing the calculation of the electron energy distribution. The resulting spectrum is presented in Fig. 4(b). One can see that there is a relatively large tail of photons with energies >20 keV, which can be used for imaging the exploding wire in water.

B. X-ray images

The PI-LCX x-ray camera used in these experiments has a detection capability for x-ray photons in the range of 0.7–25 keV. Tungsten wires were used to test the resolution of the x-ray source. Images of a 0.2 mm Tungsten wire, placed approximately 20 cm from both the x-ray source and camera, were recorded with and without using external magnetic field produced by the Helmholtz coils (see Fig. 5). In addition, a 0.2 mm diameter pinhole was placed instead of the Tungsten wire, in order to obtain the image of the x-ray source. In both cases, it can be seen that the magnetic field significantly increases the density of electrons reaching the tip of the anode, and respectively the contrast and quality of the images. This can be observed through the brightness of the pinhole image obtained in experiments with application of the magnetic field. In this case the intensity of the image is approximately 6 times higher than the intensity of the image without the magnetic field [see Figs. 5(a)–5(d)]. Let us note that although the x-ray intensity was measured in arbitrary units, the intensities shown in Figs. 5(c) and 5(d) were measured using the same calibration procedure and, therefore, are comparable. Also, it can be seen that the longitudinal distribution of x-rays incident on the anode has been greatly decreased and focused in the case of applying the magnetic field (Figs. 5(c) and 5(d)). Let us note that the minimal size of the image possible due to the pinhole size is 0.4 mm, of the order of the apparent image. Therefore, it is possible that the actual spot size on the anode was smaller than shown in the images

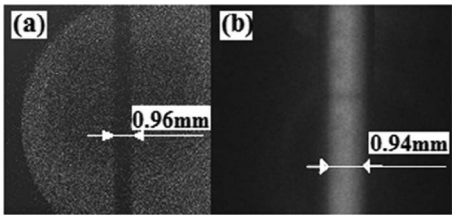

FIG. 6. Images of exploding Cu wire at time delay of 1.7 μs with respect to the beginning of the discharge current. (a) X-ray backlighting image; (b) self-light optical image.

[Figs. 5(a) and 5(b)]. It can be seen from the shadowgraph images [Figs. 5(e) and 5(f)] and the resulting intensity distributions [Figs. 5(g) and 5(h)] that the magnetic field increases the contrast of the shadow image. This can be seen from the ratio between the background x-ray signal and the dip in intensity at the wire position. With the magnetic field the intensity at the dip was attenuated to 25% of the background signal, whereas without the magnetic field the intensity was attenuated only to 55% of the background signal.

Images of the exploding 0.6 mm-diameter Cu wire were taken at different time delays with respect to the beginning of the discharge current through the wire (see Fig. 6). The x-ray and self-light images were synchronized through matching of the CVR and 4 Quik E output signals. In Fig. 7 it can be seen that the latter signals were simultaneous in time, since the beginning of the CVR signal corresponds to the time of the x-ray pulse, as shown in Fig. 4. Let us note that in most of the shots the external magnetic field was not applied. Nevertheless, the boundary of the wire can be clearly observed and measured. The resulting space resolution in this case is approximately 100 μm (see Fig. 8), derived from the 10%–90% dip in the measured x-ray intensity, and thus, the error in boundary measurement is typically ~10%.

Figure 9 presents the diameter of the wire measured through x-ray and optical images during the time evolution of the exploding wire. It can be seen that both methods result in very similar results. It is thus confirmed that self-light measurement is a sufficiently accurate method for obtaining the diameter of the exploding wire, i.e., the change in the apparent size of the wire due to optical distortion caused by the SW generated in the water and the compressed water behind it is less than 10%. In addition, the x-ray images confirmed

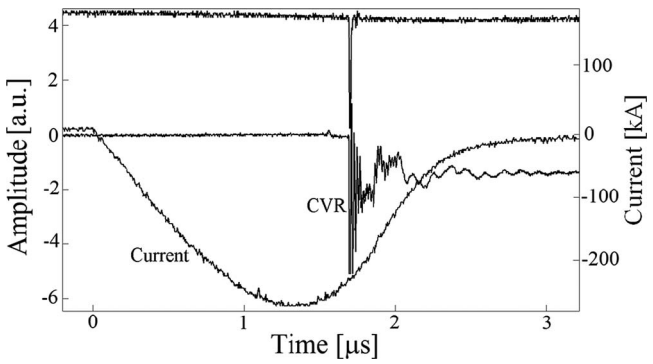

FIG. 7. Discharge current (right axis), and CVR and 4 Quik signals (left axis).

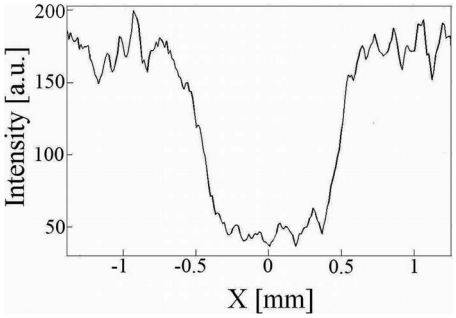

FIG. 8. X-ray intensity profile of shadowgraph of exploding Cu wire at time delay of 1.7 μs with respect to the beginning of the discharge current.

the axial uniformity of the external exploding wire boundary, for spatial scales of 0.1 mm and above. However, the resolution obtained in the x-ray images is not sufficient for measurement of small scale variations in the wire density. Let us note that thermal and magneto-hydrodynamic instabilities that typically appear during wire explosions in vacuum and air are of the scale of several μm.[14] Thus, these instabilities cannot be observed at the resolutions obtained in these experiments.

IV. ELECTRON BEAM SIMULATION

In order to model the x-ray source numerically, the ESTAT, PERMAG, and TRAK modules of the FIELD PRECISION software package[15] were used to calculate the electric field, magnetic field, and resulting electron trajectory, respectively, inside the diode. The chosen radius of the tip of the cathode and anode was 3 μm. The chosen inter-electrode gap was 1 mm and the chosen cathode potential was constant at -100 kV. The magnetic field was calculated according to the placement of the Helmholtz coils at the corresponding positions in the experiment. The simulation was performed for two cases: (1) without a magnetic field, and (2) with a current of 7.5 kA applied to the coils, resulting in an axial magnetic field of $\sim$2.2 T at the z axis. The radial component of the magnetic field was less than 5% of the total intensity. Two cases of electron emission were also chosen: field emission and space-charge limited Child-Langmuir law emission. It was found that

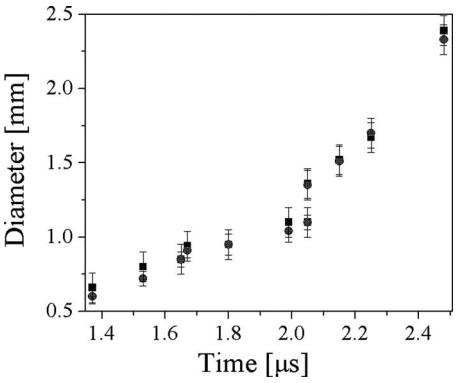

FIG. 9. Measured diameter of the exploding wire at different time delays with respect to the beginning of the discharge current. Squares denote x-ray measurements and circles denote fast frame images.

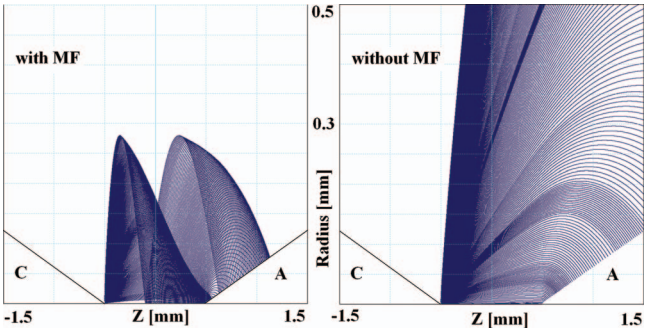

FIG. 10. Simulated trajectory of the electrons from the cathode emission according to FIELD PRECISION software. Left figure: without magnetic field, right figure: with 7.5 kA applied current to coils (2.2 T magnetic field at axis). C – Cathode, A – Anode.

the electron trajectory did not differ significantly between the two cases. The calculated electric field distribution showed that electric field at the cathode surface reaches 8 $\times$ 10^9 V/m. At that location, the field emission allows electron emission with a current density up to $\sim 10^{12}$ A/cm^2. The chosen emission surface of the cathode was the area with an electric field of $E > 3 \times 10^9$ V/m. Indeed, following field Fowler–Nordheim law[16] and accounting Schottky effect, one can calculate that at external electric field of $E = 2 \times 10^9$ V/m, the electron current density emitted from the Tungsten cathode (work function $W_w \simeq 4.5$eV) is:[17] $j_e[\mathrm{A/m^2}] = 6.2 \cdot 10^{-6} W_B^{-1} [W_F / W_w]^{1/2} E^2 \exp[-6.8 \cdot 10^9 W_w^{3/2} / E] \simeq 5\mathrm{A/m^2}$, where $W_F = 15.71$ eV is the Fermi energy, and reaches $j_e \simeq 10^8$A/cm^2 at $E = 4 \cdot 10^9$ V/m. Fig. 10 presents the trajectory of the electrons from the cathode emission surface. The size of the spot on the anode and the resolution of x-ray images are greatly influenced by the longitudinal distribution of electron impact on the anode (right side of Fig. 10). It can be seen that the trajectory differs significantly when a sufficiently strong magnetic field is applied. For the case of an applied magnetic field, although electrons reach a radius of $\sim$70 μm, the main part of the beam hits the anode at a radius of $<$20 μm, limiting the spot size to less than 40 μm. The electrons reaching larger radii complete a second oscillation around the corresponding Larmor radius. In the absence of a magnetic field, the electrons are scattered throughout a large area of the anode surface. Furthermore, the region of the highest current density of the beam, which is centered at the anode tip, is several times greater in size and smaller in current density than when a magnetic field is applied (see Fig. 10). These results are consistent with the experimental results presented in Fig. 5.

V. SUMMARY

A space- and time-resolved tabletop hard x-ray source was developed and used as a backlighting source for an underwater exploding wire. A 4 ns hard x-ray pulse was obtained, which allowed imaging of an exploding wire with a space resolution of 0.1 mm. It was shown that the applied pulsed magnetic field significantly improves the quality and contrast of the x-ray images. Results show that the wire boundary

measured by the x-ray backlighting fits well with the self-light imaging measurement. In addition, it can be seen that within the resolution limit the wire expands uniformly. This result provides further evidence of the axial uniformity of wires exploding in water. Simulations of the electron beam in the diode show that the resolution and contrast of x-ray images can be improved significantly through proper choice of parameters. Such results may be obtained with the use of a rigid, reinforced dielectric holder that can withstand the magnetic pressure generated during operation of pulsed, high current Helmholtz coils. The diode operation is currently being optimized in order to improve the resolution and intensity of the x-ray pulse.

[1]V. E. Fortov and I. T. Iakubov, *The Physics of Non-Ideal Plasma* (World Scientific, Singapore, 2000).
[2]G. S. Sarkisov, S. E. Rosenthal, K. R. Cochrane, K. W. Stuve, C. Deeney, and D. H. McDaniel, Phys. Rev. E **71**, 046404 (2005).
[3]A. W. DeSilva and J. D. Katsouros, Phys. Rev. E **57**, 5945 (1998).
[4]S. V. Lebedev, F. N. Beg, S. N. Bland, J. P. Chittenden, A. E. Dangor, M. G. Haines, M. Zakaullah, S. A. Pikuz, T. A. Shelkovenko, and D. A. Hammer, Rev. Sci. Instrum. **72**, 671 (2001).
[5]D. Sheftman and Ya. E. Krasik, Phys. Plasmas **17**, 112702 (2010).
[6]A. V. Fedotov-Gefen and Ya. E. Krasik, J. Appl. Phys. **106**, 093303 (2009).
[7]S. I. Tkachenko, A. R. Mingaleev, V. M. Romanova, A. E. Ter-Oganes'yan, T. A. Shelkovenko, and S. A. Pikuz, Plasma Phys. Rep. **35**, 734 (2009).
[8]G. Cooperstein, J. R. Boller, R. J. Commisso, D. D. Hinshelwood, D. Mosher, P. F. Ottinger, J. W. Schumer, S. J. Stephanakis, S. B. Swanekamp, B. V. Weber, and F. C. Younga, Phys. Plasmas **8**, 4618 (2001).
[9]A. Khacef, R. Viladrosa, C. Cachoncinlle, E. Robert, and J. M. Pouvesle, Rev. Sci. Instrum. **68**, 2292 (1997).
[10]G. A. Mesyats, *Explosive Electron Emission* (URO, Ekaterinburg, 1998).
[11]D. Sheftman and Ya. E. Krasik, Phys. Plasmas **18**, 092704 (2011).
[12]F. Ruhl and G. Herziger, Rev. Sci. Instrum. **51**, 1541 (1980).
[13]C. A. Brau, J. L. Raybun, J. B. Dodge, and F. M. Gilman, Rev. Sci. Instrum. **48**, 1154 (1977).
[14]I. Oreshkin, Tech. Phys. Lett. **35**, 36 (2009).
[15]S. Humphries and T. Orzechowski, Phys. Rev. ST Accel. Beams **9**, 020401 (2006).
[16]R. H. Fowler and L. W. Nordheim, Proc. R. Soc. London, Ser. A **119**, 173 (1928).
[17]K. Simoniu, *Phusikalische Electronik* (Akademiai Kiado, Budapest, 1972).